Kinetics and dynamics of annealing during sub-gel phase formation in phospholipid bilayers

A saturation transfer electron spin resonance study

Tibor Páli, Rosa Bartucci, László I. Horváth, and Derek Marsh
Max-Planck-Institut für biophysikalische Chemie, Abteilung Spektroskopie, WD-3400 Göttingen, Germany

ABSTRACT The saturation transfer electron spin resonance (STESR) spectra of spin-labeled phosphatidylcholine have been used to follow the kinetics of conversion from the gel phase to the sub-gel phase in aqueous bilayers of dipalmitoyl phosphatidylcholine. This is a simple, well-defined model system for lipid domain formation in membranes. The integrated intensity of the STESR spectrum from the chain-labeled lipid first increases and then decreases with time of incubation in the gel phase at 0°C. The first, more rapid phase of the kinetics is attributed to the conversion of germ nuclei to growth nuclei of the sub-gel phase. The increase in STESR intensity corresponds to the reduction in chain mobility of spin labels located in the gel phase at the boundaries of the growth nuclei and correlates with the increase in the diagnostic STESR line height ratios over this time range. The second, slower phase of the kinetics is attributed to growth of the domains of the sub-gel phase. The decrease in STESR intensity over this time regime corresponds to exclusion of the spin-labeled lipids from the tightly packed sub-gel phase and correlates quantitatively with calibrations of the spin label concentration dependence of the STESR intensity in the gel phase. The kinetics of formation of the sub-gel phase are consistent with the classical model for domain formation and growth. At 0°C, the half-time for conversion of germ nuclei to growth nuclei is ~7.7 h and domain growth of the sub-gel phase is characterized by a rate constant of 0.025 h^{-1}. The temperature dependence of the STESR spectra from samples annealed at 0°C suggests that the subtransition takes place via dissolution of sub-gel phase domains, possibly accompanied by domain fission.

INTRODUCTION

In addition to the transitions associated with the usual gel and fluid lamellar phases exhibited by phospholipid bilayers, it is now well known that aqueous dispersions of saturated diacyl phosphatidylcholines exhibit an additional thermotropic transition, arising from conversion to the lamellar crystalline (or sub-gel) phase on prolonged incubation at low temperatures (1, 2). Because of the slow rate of formation of the sub-gel phase, this process has been used for detailed studies of the kinetics of domain formation (3–6). There is currently much interest in the possibility of lipid domain formation in biological membranes (e.g., 7, 8), and studies on the sub-gel phase of phosphatidylcholines provide a ready model from which to obtain quantitative information on the mechanism of such processes. Although it is unlikely that sub-gel lipid structures exist in biological membranes, the kinetics of lipid domain formation may well be very similar, albeit on a different time scale, and therefore can contribute to an understanding of the biologically relevant process.

The formation of the sub-gel phase has been studied by differential dilatometry of aqueous dipalmitoyl phosphatidylcholine (DPPC)[1] dispersions and was demonstrated to occur by nucleation (3). Comparison of the degree of phase conversion on incubations at different temperatures has suggested that the processes of nucleation and growth are favored by different temperatures of incubation (5). By incubating first at lower temperature to initiate nucleation, followed by a temperature jump to higher temperature, it was possible to study the kinetics of domain growth in the absence of complications from the nucleation process (6). In the latter work, it was found that the growth of domains of the DPPC sub-gel phase occurred according to classical kinetics, but with a low fractional dimensionality, close to one. On the other hand, it has been suggested that the reverse process, i.e., the thermotropic conversion of the sub-gel phase to the gel phase at the subtransition, might occur by a rather different mechanism (9).

In the present work, the processes of both nucleation and domain growth of the sub-gel phase have been studied for DPPC bilayers by saturation transfer electron spin resonance (STESR) spectroscopy of an incorporated phosphatidylcholine spin label. This was done by incubation at a relatively low temperature (0°C) for which the nucleation rate is reasonably rapid. The STESR spectra are sensitive not only to the slow rates of chain rotation in the gel phase (10), but also, via the effects of spin–spin interactions, to the local concentrations of the spin label in the coexisting phases, even at relatively low mole fractions in the gel phase (11). It is found that these two different sensitivities of the spectra

T. Páli's and L. I. Horváth's permanent address is Institute of Biophysics, Biological Research Centre, Hungarian Academy of Sciences, P.O. Box 521, H-6071 Szeged, Hungary. R. Bartucci's permanent address is Department of Physics, University of Calabria, I-87036 Arcavacata di Rende, Italy.
Address correspondence to Derek Marsh.

[1] Abbreviations used in this paper: CW, continuous wave; DPPC, 1,2-dipalmitoyl-*sn*-glycero-3-phosphocholine; ESR, electron spin resonance; 5-PCSL, 1-acyl-2-[5-(4,4-dimethyloxazolidine-*N*-oxyl)stearoyl]-*sn*-glycero-3-phosphocholine; 5-SASL, 5-(4,4-dimethyloxazolidine-*N*-oxyl)stearic acid; STESR, saturation transfer ESR; V_1, first harmonic ESR absorption signal detected in phase with respect to the field modulation; V'_2, second harmonic absorption ESR signal detected 90° out-of-phase with respect to the field modulation.

0006-3495/93/06/1781/08 $2.00

make it possible to distinguish the nucleation and domain growth, since they are found to have opposite effects on the integrated intensity of the STESR spectra. The results obtained for the degree of conversion in the domain growth phase are found to be in quantitative agreement with independent calibrations of the spin label concentration dependence of the spectral intensities, confirming that the spectral sensitivity arises from the exclusion of the spin label from the growing domains of the sub-gel phase. The STESR studies therefore provide a direct confirmation of the formation of the sub-gel phase by nucleation with subsequent growth of domains. In addition, studies of the temperature dependence of samples in the sub-gel phase provide information on the reverse transformation occurring at the bilayer subtransition.

MATERIALS AND METHODS

Materials

DPPC was obtained from Fluka AG (Buchs, Switzerland). The spin-labeled phosphatidylcholine (5-PCSL) was synthesized from the corresponding spin-labeled stearic acid (5-SASL) as described in reference 12. The purity of the spin-labeled phospholipid was checked by thin-layer chromatography. Other chemicals used were of analytical grade purity.

Sample preparation

DPPC and spin-labeled lipid were codissolved at the desired mole ratio (200–12.5:1) in $CHCl_3/CH_3OH$ (1:2 [vol/vol]) and the solvent was then evaporated under nitrogen. The dry mixture was kept under vacuum overnight and was then dispersed at a concentration of 10 mg/ml in argon-saturated distilled water by vortex mixing at 60°C for 30 s. Aliquots of the lipid suspensions were loaded into 100-μl, 1-mm diameter glass capillaries flushed with argon and were centrifuged at 2,500 rpm for 10 min in a bench centrifuge. Excess supernatant was removed to obtain lipid pellets of 5 mm length, sealed under argon. This standardized sample configuration was used in all conventional and STESR measurements (cf., 13, 14). The samples were incubated at 60°C for 30 min, cooled to 0°C, and kept at this temperature for the desired time before the experiment.

Electron spin resonance (ESR) spectroscopy

ESR spectra were recorded at a frequency of 9 GHz on a spectrometer (model E-12 Century Line; Varian Analytical Instruments, Sunnyvale, CA) equipped with nitrogen gas flow temperature regulation and interfaced to a PDP 11/10 laboratory computer. Sample capillaries were centered in a standard 4-mm-diameter quartz tube which contained light silicone oil for thermal stability. Conventional, first harmonic, in-phase, absorption spectra (V_1 display) were recorded at a modulation frequency of 100 kHz and modulation amplitude of 0.125 mT pp, with an average microwave field over the sample of $\langle H_1^2 \rangle^{1/2} = 0.0032$ mT for low power and 0.025 mT for high power. Continuous wave (CW) saturation experiments were performed in the V_1 mode and the microwave field dependence of the amplitude, S, of the low-field hyperfine peak in the ESR powder pattern was fitted to the following expression:

$$S = S_0 \langle H_1^2 \rangle^{1/2} / (1 + \gamma^2 \langle H_1^2 \rangle T_1 T_2)^p, \qquad (1)$$

where S_0 is independent of H_1, γ is the electron gyromagnetic ratio, and T_1, T_2 are the effective longitudinal and transverse relaxation times, respectively. It was assumed that $p = 1$, corresponding to homogeneous broadening (15). Details of the determination of H_1 and the calibration of the spectrometer are given in reference 13. STESR spectra were recorded in the second harmonic, 90°-out-of-phase absorption mode (V'_2 display) at a modulation frequency of 50 kHz and a modulation amplitude of 0.5 mT pp. The phase was set by the self-null method (16) at a subsaturating microwave field of <0.0032 mT. All STESR spectra were recorded with an average microwave field at the sample of $\langle H_1^2 \rangle^{1/2} = 0.025$ mT, according to a standardized protocol for dealing with cavity Q variations and field inhomogeneities (13, 14). The normalized integral intensities of the STESR spectra were evaluated as described in reference 17. Calibrations for determination of the effective rotational correlation times from the STESR spectra were taken from reference 18. The reference spectra in reference 18 were recorded from spin-labeled hemoglobin undergoing isotropic rotational diffusion. The relation of the effective correlation times deduced from these calibrations to the anisotropic rotational diffusion of spin-labeled lipid molecules in gel phase lipid bilayers has been characterized both theoretically (19) and experimentally (15, 20).

RESULTS

Spectral effects of incubation at 0°C

Samples of fully hydrated DPPC containing the 5-PCSL phosphatidylcholine spin label at a mole ratio of 1:200 were incubated at 0°C for periods of up to 200 h to follow the changes in the ESR spectrum on formation of the sub-gel phase. Saturation transfer ESR spectra (V'_2 display) recorded during progressive incubation are given in Fig. 1. The corresponding conventional ESR spectra (data not shown) reveal only slight increases in the spectral line widths, without change in the outer hyperfine splitting, with time of incubation at 0°C. The STESR spectra show modest changes in line shape with increasing time of incubation at 0°C that are characterized by the diagnostic spectral line height ratios that are given in Fig. 2. The principal change in the line height ratios takes place over the range of incubation times from 0 to 5 h and reaches a broad maximum after times of ~20–25 h. These changes are essentially consistent with those obtained over the same time range with phosphatidylcholine spin labeled at the sixth position (15), except that the initial values of the central line height ratio were lower for the latter label position. Beyond incubations of ~25 h, the line height ratios decrease slightly but steadily with further incubation. The effective rotational correlation times deduced from the diagnostic line height ratios by using the calibrations of reference 18 are given in Table 1. Different values are obtained from the C′/C ratios than those from the L″/L and H″/H ratios because the lipid motion is anisotropic, whereas the calibrations are for isotropic motion (15, 19). The lower value deduced from C′/C suggests a preferentially faster rotation about the long axis of the lipid molecule (20). It is noted that the line height ratios given in Table 1 are still in a region that is sensitive to both axial and off-axial motion; higher values would be expected for all ratios if the spin-labeled lipid actually fully entered the (crystalline) sub-gel phase (cf., 10 and 20).

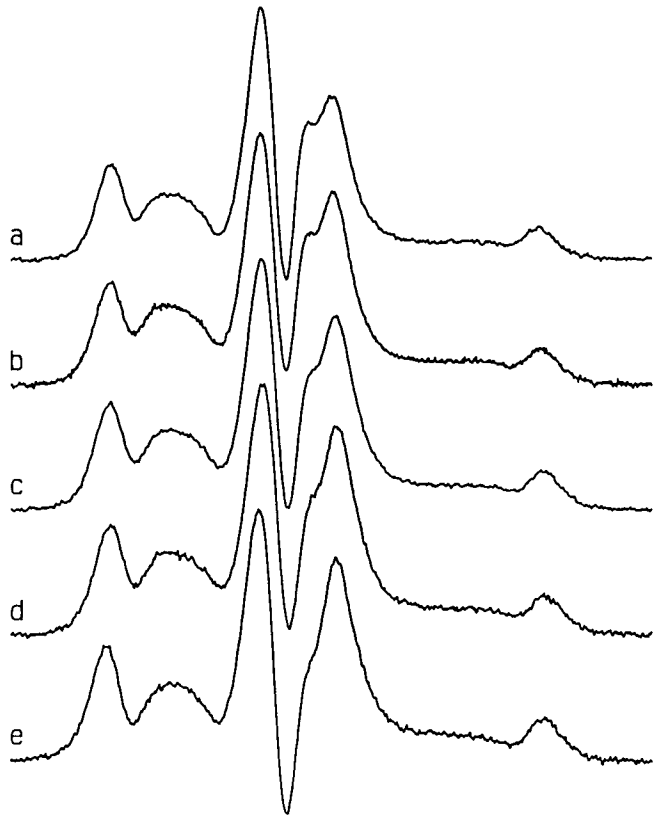

FIGURE 1 Second harmonic, out-of-phase STESR spectra (V'_2 display) of 5-PCSL (0.5 mol%) in fully hydrated DPPC dispersions incubated at 0°C for increasing periods of time: (*a*) 1.3 h, (*b*) 8.7 h, (*c*) 32 h, (*d*) 58 h, and (*e*) 105 h. Spectra are normalized to the maximum line height; the vertical expansion factors relative to normalization to the integrated intensity are: (*a*) 1.00, (*b*) 0.96, (*c*) 1.12, (*d*) 1.45, and (*e*) 1.78. Total scan width = 10 mT; T = 0°C.

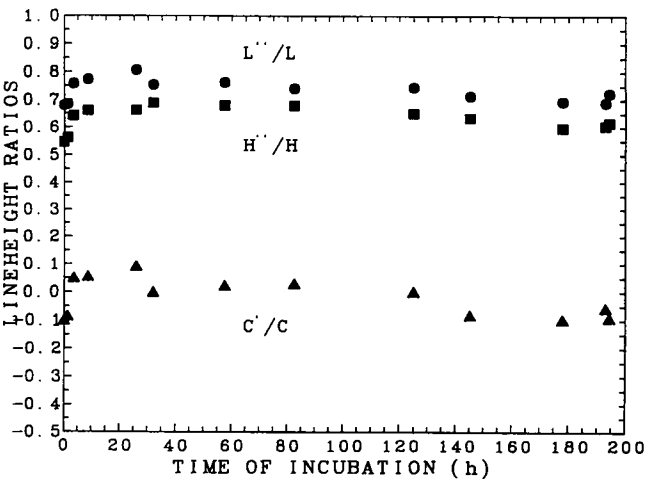

FIGURE 2 Dependence of the diagnostic line height ratios in the STESR spectra of 5-PCSL (0.5 mol%) in aqueous DPPC dispersions on time of incubation at 0°C. (●) low-field ratio, L″/L; (■) high-field ratio, H″/H; (▲) central ratio, C′/C. T = 0°C.

The STESR spectra shown in Fig. 1 are normalized with respect to their maximum line height and do not reflect the rather considerable changes in spectral intensity that take place on prolonged incubation at 0°C. The time dependence of the reciprocal STESR integral intensity with increasing duration of incubation of the sample at 0°C is given in Fig. 3. The dependence on the incubation time is reproducibly biphasic with an initial, faster decrease in the reciprocal saturation transfer integral accompanied by a slower increase that comes to dominate at longer times of incubation. The clearly biphasic response in Fig. 3 has been fitted to the following kinetic equation (see Discussion):

$$1/I_{ST} = A_1/I^i_{ST}/[A_1 + 1 - \exp(-k_1 t)] + A_2 \cdot C/[A_2 - 1 + \exp(-k_2 t)] - C, \quad (2)$$

where the first term represents the phase with decreasing $1/I_{ST}$ and the second term represents the phase with increasing $1/I_{ST}$. A nonlinear least-squares fit to Eq. 2 yields the following values for the amplitude parameters: $A_1 = 2.9$, $A_2 = 1.32$, $C = 127$, and $1/I^i_{ST} = 355$, and the rate constants: $k_1 = 0.09\ h^{-1}$, $k_2 = 0.033\ h^{-1}$. The kinetic parameters for the first phase are determined with less accuracy than those for the second phase because of the limited interval over which the first phase is dominant.

Spectral effects of spin label concentration

To determine the effects of possible increases in the local spin label concentration, the STESR spectra were recorded for samples with increasing mole fraction of the 5-PCSL spin label in DPPC bilayers in the gel phase at 0°C. In contrast to the diagnostic line height ratios (data not shown), it was found that the STESR integral inten-

TABLE 1 **Effective rotational correlation times, τ_R, of the 5-PCSL spin label in DPPC dispersions obtained from calibrations for the diagnostic STESR line height ratios, L″/L, C′/C, and H″/H***

	τ_R (μs)		
	L″/L	C′/C	H″/H
Time of incubation at 0°C (h)			
0	37	3.5	54
25	44	5.5	78
196	38	3.5	66
Dependence on temperature (°C)			
10	41	3.8	78
16	46	5.2	93
27	44	4.2	72
33	47	0.06	59
39	51	0.04	54

* Reference spectra were taken from spin-labeled hemoglobin (18). The uncertainties in the line height ratios were approximately ±3.5, ±2, and ±10% for L″/L, C′/C, and H″/H, corresponding to ±2.5, ±0.01, and ±12 μs in effective correlation time, respectively.

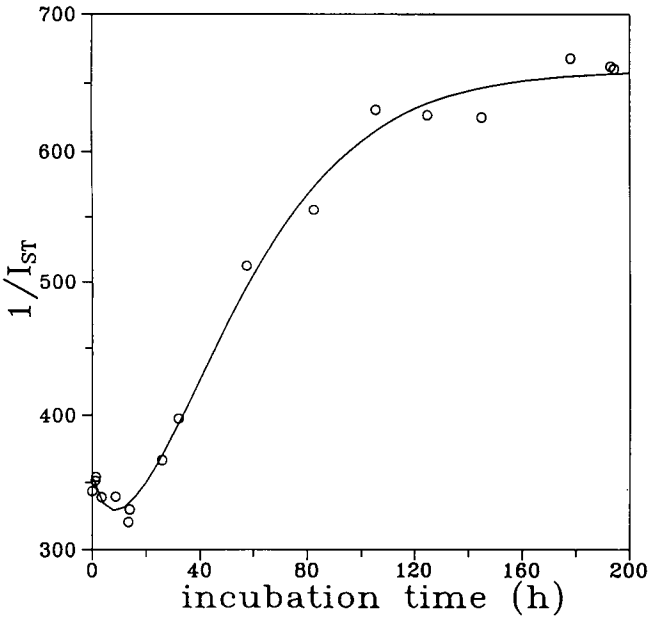

FIGURE 3 Dependence of the reciprocal saturation transfer integral, $1/I_{ST}$, of the 5-PCSL phosphatidylcholine spin label (0.5 mol%) in aqueous dispersions of DPPC on time of incubation at 0°C. The solid line represents a non-linear least-squares fit to Eq. 2. T = 0°C.

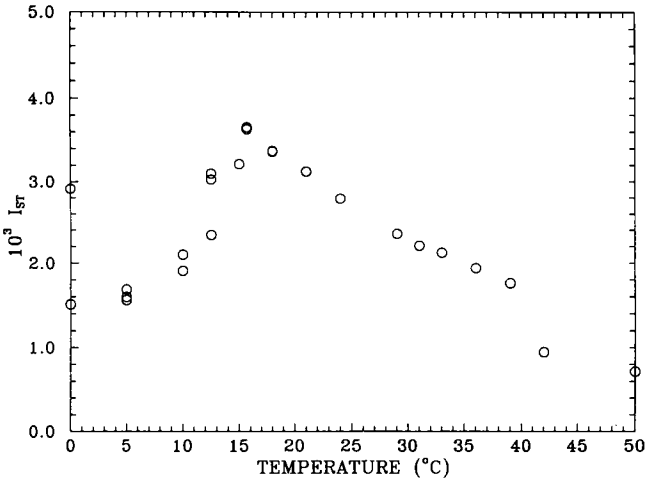

FIGURE 5 Temperature dependence of the saturation transfer integral, I_{ST}, of fully hydrated DPPC dispersions labeled with 5-PCSL, at a mole fraction of 0.5%. Multiple points in the region 5–15°C indicate the time dependence at the individual temperature points during the temperature dependence. In each case, the lowest point is the initial measurement and the values then increase, overlapping as equilibration is achieved. The lower point at 0°C is after incubation, and the upper point is recorded immediately after cooling from 50°C at the end of the temperature run. The latter is identical to that recorded initially, before the incubation at 0°C.

sity, which is given in Fig. 4, depends strongly on spin label concentration (cf., 11, 21). Over the range studied in Fig. 4, the concentration dependence of the reciprocal saturation transfer integral can be approximated by the following linear form:

$$1/I_{ST} = 1/I^0_{ST} + a \cdot c, \qquad (3)$$

where c is the mole fraction of spin label, $1/I^0_{ST}$ is the reciprocal STESR intensity extrapolated to zero concentration, and a is a constant determined by the strength of the effectively bimolecular spin–spin interactions. The linear-regression parameters, a = 25240 and $1/I^0_{ST}$ = 256, obtained from Fig. 4 serve to calibrate the spin label concentration from measurements of the STESR integral intensity, for example in situations with mixed phases that are dealt with in the Discussion.

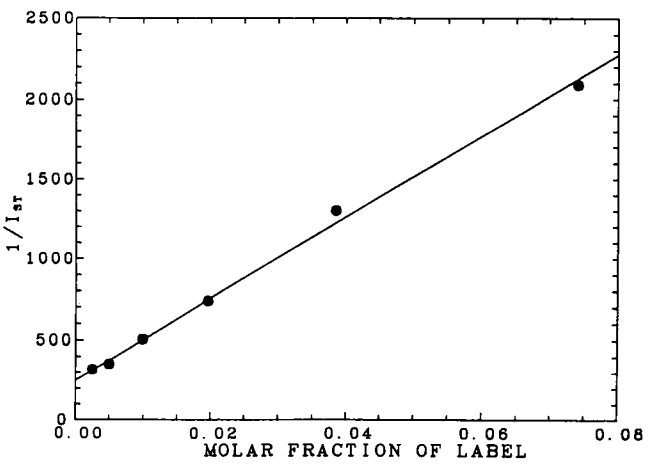

FIGURE 4 Dependence of the reciprocal saturation transfer integral, $1/I_{ST}$, of the 5-PCSL spin label on the mole fraction of the spin-labeled phosphatidylcholine in aqueous dispersions of DPPC in the gel phase at T = 0°C. The solid line represents a linear regression to Eq. 3.

CW saturation experiments were also carried out to confirm that the dependence of the reciprocal saturation transfer integral on the mole fraction of spin label corresponded to the expected effect of spin–spin interactions on the spin label relaxation (cf., reference 11). The reciprocal effective T_1T_2 product was found to depend linearly on the mole fraction of spin label over the same range as that shown in Fig. 4 (data not shown). This result is consistent with a linear dependence of the relaxation rate on c, with the relative effects on T_1 dominating those on T_2, thus confirming the proportionality between saturation transfer intensity and effective spin-lattice relaxation time (cf., 22).

Temperature dependence of the STESR spectra

DPPC dispersions containing 0.5 mol% of the 5-PCSL spin label were incubated for long times at 0°C to reach the equilibrium level indicated in Fig. 3. The temperature dependence of the integral of the saturation transfer spectrum on heating after this incubation is given in Fig. 5. The temperature was changed between measurement points at an effective rate of ~0.2°/min and, where necessary, the sample was further incubated at the given

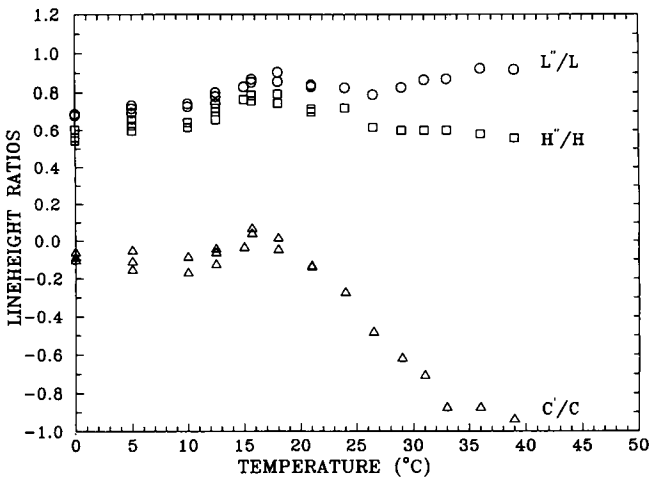

FIGURE 6 Temperature dependence of the diagnostic line height ratios from the saturation transfer spectra of fully hydrated DPPC dispersions labeled with 5-PCSL, at a mole fraction of 0.5%. (○) low-field ratio, L″/L; (□) high-field ratio, H″/H; (△) central ratio, C′/C. Multiple points in the region 0–15°C indicate the time dependence at the individual temperature points during the temperature dependence. At 5°C, the line height ratios first increase and then decrease to lower than the initial value; at all other temperatures the values increase with time of incubation, except at 18°C, where they decrease.

temperature with repetitive recording of the STESR spectrum. The two data points given at 0°C correspond to the decrease in I_{ST} observed from before to after the incubation period. The multiple data points given for the individual temperatures indicated in the range 0–15°C represent the relaxation of the system to the new equilibrium (increasing I_{ST}) in the sub-gel phase after the increase in temperature. In general, the saturation transfer integral is found to increase with increasing temperature up to the subtransition at ~14–15°C. Beyond this temperature, the values of I_{ST} decrease with increasing temperature in the gel phase; also the rate of attainment of equilibrium at the new temperature was much faster (within the effective scan rate) and no time dependence of the spectra was observed. Beyond 25–30°C, the temperature dependence of the saturation transfer integral is seen to decrease, corresponding to the passage through the pretransition to the intermediate, rippled ($P_{\beta'}$) gel phase. The main, chain-melting phase transition is accompanied by a further, sharp decrease in the saturation transfer integral at ~40°C, going from the gel phase to the fluid (L_α) phase.

The diagnostic line height ratios in the STESR spectrum (given in Fig. 6) display relatively little temperature dependence in the sub-gel phase. Small increases are observed with increasing temperature up to the subtransition, as indicated by the effective rotational correlation times deduced from the low-field, central, and high-field ratios (L″/L, C′/C, and H″/H, respectively) recorded at different temperatures that are given in Table 1. These small changes indicate that the rather large increases in the saturation transfer integral with increasing temperature in the sub-gel phase that are shown in Fig. 5 arise primarily from a decrease in spin–spin interactions between spin labels (cf., Fig. 4), rather than from changes in rotational mobility of the spin-labeled lipid chains. The low- and high-field line height ratios, L″/L and H″/H, also do not change greatly with increasing temperature in the gel phase above the subtransition (cf., Table 1), whereas the central ratio, C′/C, decreases steeply in the region around 25°C, corresponding to the onset of more rapid axial chain rotations in the $P_{\beta'}$, ripple phase, as found previously (20). This is further indicated by the increased difference (i.e., anisotropy) between the effective rotational correlation times deduced from the C′/C ratios and those from the L″/L and H″/H ratios that is evident from Table 1.

The STESR spectra recorded on cooling to 0°C immediately after the temperature variation experiment were identical to those obtained initially before the incubation at 0°C and subsequent temperature variation. This reversibility indicates that the lipid membranes were stable throughout the lengthy incubation and also during the following temperature variation. It should be noted that the incubation was carried out at low temperature, whereas the period of exposure to the higher temperatures was relatively short, also the samples were under argon.

DISCUSSION

Chain mobility and domain formation in the sub-gel phase

The relaxation of the gel phase to the sub-gel phase is characterized by biphasic changes in the STESR integral intensity of the incorporated spin-labeled phosphatidylcholine (see Fig. 3). The initial phase, in which $1/I_{ST}$ decreases, correlates quantitatively in magnitude and approximately in time span with the increase in the STESR diagnostic line height ratios (Fig. 2 and see later text), and corresponds to a decrease in rotational mobility of the spin-label on nucleation of the sub-gel phase (cf. e.g., 23). The subsequent large increase in $1/I_{ST}$ does not correspond to a change in the spin-label mobility, since the diagnostic STESR line height ratios do not change greatly over this time regime (see Fig. 2), even though the STESR spectral line shapes lie in a regime that is sensitive to such changes (cf., 10, 15, 20). The small decrease that is observed in the line height ratios would correspond only to a small increase in $1/I_{ST}$, if this were due to an increase in rotational mobility. Therefore, the large increase observed in $1/I_{ST}$ must correspond to an increase in the local concentration of the spin label (as characterized by the concentration dependence given in Fig. 4) due to exclusion of the spin label from the growing domains of the sub-gel phase (cf., 15, 24). It will be noted also that a decrease in the STESR intensity with-

out appreciable change in line shape is a characteristic feature of spin–spin interactions (11, 21). The fact that $1/I_{ST}$ reaches a limiting value, rather than diverging at long times, suggests that a proportion of the gel phase, namely that corresponding to intervening regions between the colliding domains of the sub-gel phase, remains unconverted. Such an effect has been observed previously in dilatometric studies of the relaxation to the sub-gel phase in DPPC at 0.5°C (5).

Kinetics of sub-gel nucleation and domain growth

The kinetics of relaxation of the STESR integral intensity shown in Fig. 3 can be interpreted on the above basis in terms of the formation of sub-gel phase nuclei of critical size followed by domain growth (cf., 3, 5, 6). The production of nuclei of critical size from preexisting germ nuclei within the gel phase follows first order kinetics, if the rate is sufficiently rapid compared with the domain growth (and the concentration of germ nuclei is sufficiently low) that the removal of germ nuclei by the enveloping domain growth may be neglected (cf., 25):

$$N = N^0[1 - \exp(-k_1 t)], \tag{4}$$

where N is the concentration of growth nuclei, N^0 is the initial concentration of germ nuclei, and k_1 is the rate of conversion of germ nuclei into nuclei of critical size. Further, if the rate of domain growth is sufficiently slow that it may be assumed to a first approximation that essentially all of the germ nuclei have been converted to growth nuclei, the rate of conversion to the sub-gel phase by domain growth is given by (cf., 6, 26):

$$dX/dt = N^0[1 - X/X^\infty]dV_1/dt, \tag{5}$$

where X is the degree of conversion, V_1 is the domain size corresponding to unrestricted growth, and the term $[1 - X/X^\infty]$, allows for the complication of domains meeting. The excluded volume between domains that was referred to above is included by the factor $1/X^\infty$, where X^∞ is the final, limiting degree of conversion. Assuming a constant linear growth rate, u, in domain size, the value of V_1 is given by:

$$V_1 = gu^n t^n, \tag{6}$$

where g is a geometrical factor depending on the directionality of the growth in domain shape and n is the dimensionality of domain growth. Yang and Nagle (6) found that $n \approx 1$ for the domain growth of the sub-gel phase in DPPC. Integrating the rate equation (Eq. 5) then yields the following expression for conversion to the gel phase by domain growth:

$$X = X^\infty[1 - \exp(-k_2 t)], \tag{7}$$

where $k_2 = (N^0/X^\infty)gu$ and it is assumed that $n = 1$.

It remains to relate the changes in the saturation transfer integral to the production of growth nuclei and the degree of conversion to the sub-gel phase that are given by Eqs. 4 and 7, respectively. Since the STESR integral is additive in multicomponent systems (17), the change in I_{ST} corresponding to creation of growth nuclei will be related linearly to the degree of production, N/N^0. The resulting change in $1/I_{ST}$ due to nucleation is:

$$\Delta(1/I_{ST})_{nucl} = \{1/[1 + (I_{ST}^\infty/I_{ST}^i - 1)N/N^0] - 1\}/I_{ST}^i, \tag{8}$$

where I_{ST}^∞ and I_{ST}^i are the final and initial values of the STESR integral corresponding to $N = N^0$ and $N = 0$, respectively. The change in $1/I_{ST}$ resulting from domain growth will be related linearly to the mole fraction, c, of spin-label concentrating in the gel phase as a result of exclusion from the domains of the sub-gel phase (cf., Eq. 3). This increase in mole fraction of spin label in the gel phase is given by:

$$c = c_0/(1 - X), \tag{9}$$

where c_0 (=0.005) is the original total mole fraction of spin-label in the sample. From Eq. 3 for the concentration dependence of the STESR integral, the change in $1/I_{ST}$ resulting from domain growth is therefore:

$$\Delta(1/I_{ST})_{dom} = ac_0[1/(1 - X) - 1]. \tag{10}$$

The net value of $1/I_{ST}$ for the whole sample is then given by:

$$1/I_{ST} = 1/I_{ST}^i + \Delta(1/I_{ST})_{nucl} + \Delta(1/I_{ST})_{dom}. \tag{11}$$

Combining Eqs. 4, 7, 8, 10, and 11 yields a kinetic equation for $1/I_{ST}$ that is of the form given by Eq. 2, where $A_1 = 1/(I_{ST}^\infty/I_{ST}^i - 1)$, $A_2 = 1/X^\infty$, and $C = ac_0$.

It is seen from Fig. 3 that the kinetics of relaxation of the STESR integral can be fit adequately by the above model, as described by Eq. 2. The best fit value of $C = 127$ corresponds very well with the value of $ac_0 = 126.2$ predicted from the measured concentration dependence given in Eq. 3, and gives further support for the model used in describing the growth phase kinetics. The value derived for $X^\infty = 0.76$ corresponds to 24% of the gel phase remaining unconverted in the regions between the domains of sub-gel phase at long times. Tristram-Nagle et al. (5) obtained a similar limiting value of ~20% unconverted lipid from dilatometric measurements of the conversion to the sub-gel phase for DPPC incubated at 0.5°C. The value deduced for I_{ST}^∞ from the fitted parameters A_1 and I_{ST}^i corresponds to an increase in the effective rotational correlation time (cf., 17) of only 50% relative to that in the original gel phase. A similar result is obtained from the increase in the diagnostic STESR line height ratios over the same time range in Fig. 2 (cf., Table 1). Although I_{ST}^∞ is not determined to a high degree of accuracy, its low value indicates that the spin labels are located in the gel phase, i.e., at the surface of the growth nuclei rather than in their interior. Such an interpretation is consistent with the model in which the

spin labels are excluded from the growing domains. Increases in lipid chain packing density have been observed by x-ray diffraction throughout the incubation time period required for formation of the subgel phase (4, 27). This implies a general decrease of lipid chain mobility in the gel phase at short incubation times, in agreement with the present spin label results.

The rate of conversion from germ nuclei to growth nuclei is $k_1 = 0.09/\text{h}$, corresponding to a half-time of ~7.7 h at 0°C. As noted in Results, this rate is only approximate because the fit is somewhat insensitive to the parameters of the initial phase. It is interesting to note that an initial rapid phase, over a period of 5 h, has been observed for the change in the lamellar repeat spacing on incubation of DPPC at 0.5°C (27), and this initial phase is accompanied by rapid changes in the interchain spacing (cf., 4). Also, two-stage changes have been observed in the infrared spectrum of DPPC incubated at 2°C, where the first stage extends over incubation times of 9 h, possibly up to 17 h (28). Although these changes were not identified mechanistically, the time frame correlates reasonably well with that assigned here to the nucleation process.

From the rate constant k_2 characterizing domain growth a value of $N^0gu = 0.025\ \text{h}^{-1}$ at 0°C is obtained. Yang and Nagle (6) have obtained a corresponding value of 0.0045 h^{-1} (characterized by a value of $n = 1.06$) for the growth of sub-gel domains in DPPC at 10°C. The difference in these two values arises, at least in part, from the much larger number of growth nuclei, N^0, created at 0°C than in the quenching from 4.1°C used by the latter authors. The temperature dependence of the nucleation rate is determined primarily by the extent of undercooling, $T - T_S$, and for two-dimensional systems is given by the factor: $\exp[-(\Delta E + B)/kT] \exp[-B/(T - T_S)]$, where ΔE is the activation energy for nuclear growth, B is a constant depending on the energetics of formation of the growth nuclei, and T_S (=13.5°C) is the subtransition temperature (e.g., 29). At temperatures above 6°C the nucleation rate in gel-phase DPPC is extremely slow (3).

An effective first order rate constant of 0.051/h has been determined for the change in the x-ray long spacing on incubation of DPPC at 0.5°C (27). Similarly, decreases in x-ray long spacing were found to take place over a period of ~12 h for DPPC incubated at −2°C. These changes, which were identified as arising from interlamellar dehydration, are more rapid than those found here for the domain growth of the sub-gel phase. The time scale for the latter is more comparable to the incubation times required to achieve the full calorimetric enthalpy of the subtransition (4).

Temperature dependence in the sub-gel phase

The results of Fig. 5 reveal two interesting features of the temperature dependence of the saturation transfer integral in the sub-gel phase. The first is that the integrated intensity increases rather steeply with increasing temperature on approaching the subtransition, which takes place at a temperature of ~14–15°C. Since the size of the increase is greater than would be expected from the change in rotational mobility as registered by the diagnostic STESR line height ratios (see Table 1), it must arise from the decrease in local concentration of the spin label segregated into the gel phase as the sub-gel phase domains "melt" to the gel phase. Whether this is solely a function of the degree of phase conversion, or corresponds also to changes in domain size at constant phase composition (i.e., domain fission), is not known with certainty. However, the fact that the effective rotational correlation times given in Table 1 do increase somewhat with increasing temperature in the sub-gel phase (cf., also Fig. 6), which is most likely a reflection of the immobilization of the gel-phase lipid chains at the boundaries of the sub-gel domains, does give support to this latter interpretation.

The second notable aspect of Fig. 5 is the time dependence of the saturation transfer integral after an increase in temperature in the sub-gel phase. As for the domain growth, the kinetics of dissolution of the domains is also slow, being in this case on the time scale of hours, except at the subtransition where equilibration is obtained approximately within an hour. Such effects are consistent with the dependence of the subtransition temperature on scan rate, as observed in calorimetric experiments (1, 5), and also with the change in lamellar repeat spacing after a temperature jump from the sub-gel phase to the gel phase (27). Larger changes in the STESR intensity with time are observed closer to the subtransition, since here the overall change is greater.

It has been suggested, from measurements of the bilayer repeat distance, that the subtransition of DPPC takes place in a more continuous fashion, rather than with the coexistence of large-scale domains (9). However, these experiments were performed at relatively fast scan rates and were sensitive only to long-range order. It is conceivable, in cases where the degree of conversion is complete (i.e., $X^\infty = 1$), that the sub-gel to gel transition may take place without domain formation, even though domains are formed in the reverse process, viz., relaxation of the gel phase to the sub-gel phase. Nevertheless, it has been observed that the static x-ray diffraction patterns of DPPC in the subtransition region contain overlapping components, consistent with the coexistence of sub-gel and gel domains (2). Therefore it seems likely that, at equilibrium, the subtransition occurs also via domain formation, as found here for the reverse process and in agreement with the results of Fig. 5.

Conclusion

The nucleation and growth regimes of the sub-gel phase in DPPC bilayers have been observed simultaneously from the biphasic dependence of the intensity of the

STESR spectrum from an incorporated phosphatidylcholine spin-label on the time of incubation at 0°C. The ability of STESR spectroscopy to distinguish both stages in the formation of the sub-gel phase arises on the one hand from the sensitivity to slow rotational diffusion (i.e., to the chain dynamics) and on the other hand from the sensitivity to weak spin–spin interactions between labels (i.e., to the inhomogeneity of label distribution in two-phase systems). It is likely that the method may also be applied usefully to the study of lipid domain formation in other cases, e.g., those of lateral phase separation in mixed lipid systems.

T. Páli was supported by a fellowship from the Federation of European Biochemical Societies.

Received for publication 20 November 1992 and in final form 8 February 1993.

REFERENCES

1. Chen, S. C., J. M. Sturtevant, and B. J. Gaffney. 1980. Scanning calorimetric evidence for a third phase transition in phosphatidylcholine bilayers. *Proc. Natl. Acad. Sci. USA.* 77:5060–5063.
2. Füldner, H. H. 1981. Characterization of a third phase transition in multilamellar dipalmitoyllecithin liposomes. *Biochemistry.* 20:5707–5710.
3. Nagle, J. F., and D. A. Wilkinson. 1982. Dilatometric studies of the subtransition in dipalmitoylphosphatidylcholine. *Biochemistry.* 21:3817–3821.
4. Ruocco, M. J., and G. G. Shipley. 1982. Characterization of the sub-transition of hydrated dipalmitoylphosphatidylcholine bilayers: kinetic, hydration and structural study. *Biochim. Biophys. Acta.* 691:309–320.
5. Tristram-Nagle, S., M. C. Wiener, C.-P. Yang, and J. F. Nagle. 1987. Kinetics of the subtransition in dipalmitoylphosphatidylcholine. *Biochemistry.* 26:4288–4294.
6. Yang, C. P., and J. F. Nagle. 1988. Phase transformations in lipids follow classical kinetics with small fractional dimensionalities. *Phys. Rev. A.* 37:3993–4000.
7. Thompson, T. E., M. B. Sankaram, and R. L. Biltonen. 1992. Biological membrane domains: functional significance. *Comm. Molec. Cell Biophys.* 8:1–15.
8. Marsh, D. 1992. Role of lipids in membrane structures. *Curr. Opin. Struct. Biol.* 2:497–502.
9. Tenchov, B. G., H. Yao, and I. Hatta. 1989. Time-resolved x-ray diffraction and calorimetric studies at low scan rates. 1. Fully hydrated dipalmitoylphosphatidylcholine (DPPC) and DPPC/water/ethanol phases. *Biophys. J.* 56:757–768.
10. Thomas, D. D., L. R. Dalton, and J. S. Hyde. 1976. Rotational diffusion studied by passage saturation transfer electron paramagnetic resonance. *J. Chem. Phys.* 65:3006–3024.
11. Marsh, D., and L. I. Horváth. 1992. Influence of Heisenberg spin exchange on conventional and phase quadrature EPR lineshapes and intensities under saturation. *J. Magn. Reson.* 97:13–26.
12. Marsh, D., and A. Watts. 1982. Spin labeling and lipid-protein interactions in membranes. *In* Lipid-Protein Interactions. Vol. 2. P. C. Jost, and O. H. Griffith, editors. Wiley-Interscience, New York. 53–125.
13. Fajer, P., and D. Marsh. 1982. Microwave and modulation field inhomogeneities and the effect of cavity Q in saturation transfer ESR spectra. Dependence on sample size. *J. Magn. Reson.* 49:212–224.
14. Hemminga, M. A., P. A. de Jager, D. Marsh, and P. Fajer. 1984. Standard conditions for the measurement of saturation-transfer ESR spectra. *J. Magn. Reson.* 59:160–163.
15. Fajer, P., A. Watts, and D. Marsh. 1992. Saturation transfer, continuous wave saturation, and saturation recovery electron spin resonance studies of chain-spin labeled phosphatidylcholines in the low temperature phases of dipalmitoyl phosphatidylcholine bilayers. Effects of rotational dynamics and spin-spin interactions. *Biophys. J.* 61:879–891.
16. Marsh, D. 1982. Electron spin resonance: spin label probes. *Tech. Life Sci. Biochem.* B4/II, B426/1–B426/44.
17. Horváth, L. I., and D. Marsh. 1983. Analysis of multicomponent saturation transfer ESR spectra using the integral method: application to membrane systems. *J. Magn. Reson.* 54:363–373.
18. Horváth, L. I., and D. Marsh. 1988. Improved numerical evaluation of saturation transfer electron spin resonance spectra. *J. Magn. Reson.* 80:314–317.
19. Robinson, B. H., and L. R. Dalton. 1980. Anisotropic rotational diffusion studied by passage saturation transfer electron paramagnetic resonance. *J. Chem. Phys.* 72:1312–1324.
20. Marsh, D. 1980. Molecular motion in phospholipid bilayers in the gel phase: long axis rotation. *Biochemistry.* 19:1632–1637.
21. Horváth, L. I., L. Dux, H. O. Hankovszky, K. Hideg, and D. Marsh. 1990. Saturation transfer electron spin resonance of Ca^{2+}-ATPase covalently spin-labelled with β-substituted vinyl ketone- and maleimide-nitroxide derivatives. *Biophys. J.* 58:231–241.
22. Páli, T., R. Bartucci, L. I. Horváth, and D. Marsh. 1992. Distance measurements using paramagnetic ion-induced relaxation in the saturation transfer electron spin resonance of spin-labeled biomolecules. Application to phospholipid bilayers and interdigitated gel phases. *Biophys. J.* 61:1595–1602.
23. Marsh, D., and L. I. Horváth. 1989. Spin label studies of the structure and dynamics of lipids and proteins in membranes. *In* Advanced EPR Applications in Biology and Biochemistry. A. J. Hoff, editor, Elsevier, Amsterdam. 707–752.
24. Boggs, J. M., and J. T. Mason. 1986. Calorimetric and fatty acid spin label study of subgel and interdigitated gel phases formed by asymmetric phosphatidylcholines. *Biochim. Biophys. Acta.* 863:231–242.
25. Avrami, M. 1939. Kinetics of phase change. I. *J. Chem. Phys.* 7:1103–1112.
26. Avrami, M. 1940. Kinetics of phase change. II. *J. Chem. Phys.* 8:212–224.
27. Akiyama, M., N. Matsushima, and Y. Terayama. 1987. Kinetics of the subtransition of multilamellar dipalmitoylphosphatidylcholine. *Jpn. J. Appl. Phys.* 26:1587–1591.
28. Cameron, D. G., and H. H. Mantsch. 1982. Metastability and polymorphism in the gel phase of 1,2-dipalmitoyl-3-*sn*-phosphatidylcholine. A Fourier transform infrared study of the subtransition. *Biophys. J.* 38:175–184.
29. Frenkel, J. 1955. Kinetic Theory of Liquids. Dover Publications, New York, 488 pp.